

Hierarchical Liouville-space approach for accurate and universal characterization of quantum impurity systems

ZhenHua Li,¹ NingHua Tong,¹ JianHua Wei,^{1,*} Xiao Zheng,^{2,†} Jie Hu,^{3,4} and YiJing Yan^{2,3,‡}

¹*Department of Physics, Renmin University of China, Beijing 100872, China*

²*Hefei National Laboratory for Physical Sciences at the Microscale,
University of Science and Technology of China, Hefei 230026, China*

³*Department of Chemistry, Hong Kong University of Science and Technology, Hong Kong, China*

⁴*Department of Physics, Capital Normal University, Beijing 100048, China*

(Dated: July 27, 2012)

A hierarchical equations of motion based numerical approach is developed for accurate and efficient evaluation of dynamical observables of strongly correlated quantum impurity systems. This approach is capable of describing quantitatively Kondo resonance and Fermi liquid characteristics, achieving the accuracy of latest high-level numerical renormalization group approach, as demonstrated on single-impurity Anderson model systems. Its application to a two-impurity model reproduces the experimentally observed crossover behavior, which affirms the continuous transition from the Kondo singlet state of individual impurity to the singlet spin-state formed between two impurities.

PACS numbers: 71.27.+a, 72.15.Qm

Quantum impurity systems cover a broad range of important physical systems where strong electron-electron (e - e) interactions among a few localized impurities affect crucially the system properties. Besides the e - e interactions, the impurities are also coupled to the itinerant electrons in surrounding bulk materials, which serve as the electron reservoir as well as thermal bath for the impurities. Moreover, some extensive strongly correlated systems can be treated as quantum impurity systems. For instance, the celebrated Hubbard model can be mapped onto an Anderson impurity system via a self-consistent dynamical mean-field theory [1]. The strong e - e interactions give rise to a variety of intriguing phenomena of prominent many-body nature, such as Kondo effects, Mott metal-insulator transition, and high-temperature superconductivity. Examples of localized impurities are the d - or f -electrons of transition metal atoms, and electrons trapped in quantum dots.

Accurate characterization of quantum impurity systems is the key to understand the mechanisms and effects of strong electron correlations. This has remained a very challenging task, especially for the quantitative evaluation of dynamical quantities which are directly related to experimental measurements, such as the projected density of states and spectral function of the localized impurities. A vast amount of theoretical efforts have been devoted to achieving this goal. A variety of numerical approaches have been developed, including the quantum Monte Carlo approach [2], density matrix renormalization group method [3, 4], numerical renormalization group (NRG) method [5, 6], many-body perturbation theory [7], and effective/quasi single-particle approaches

[8, 9]. Despite their success in elucidating some fundamental features of strongly correlated systems, the practicality of existing approaches has been limited within a few basic models [10–12]. The reason is mainly twofold: (i) the applicability of involving techniques relies critically on the system configuration, and (ii) the complexity of numerical algorithms employed increases dramatically with the number of impurities. Consequently, generalization of existing approaches [2–6] to more complex models is often very difficult. Therefore, an accurate and universal approach capable of addressing strong correlation effects in general quantum impurity systems is highly desirable.

In this Letter we propose a general approach based on a hierarchical equations of motion (HEOM) formalism [13] to characterize quantum impurity systems from the perspective of open dissipative dynamics. Using this approach, a variety of dynamical observables of significant experimental relevance can be evaluated accurately and efficiently. We first exemplify its practicality through the evaluation of spectral functions of single-impurity Anderson model (SIAM) systems. Its accuracy is shown to be comparable to the latest high-level NRG approach. The associated Kondo resonance and Fermi liquid characteristics are scrutinized by comparing directly to existing numerical and analytical results. Calculations are then extended to a two-impurity Anderson model (TIAM) system, where unconventional Kondo resonance features is disclosed which well reproduces a recent experiment [14].

In the framework of HEOM, the localized impurities constitute the open system of primary interest, while the surrounding reservoirs of itinerant electrons are treated as environment. The total Hamiltonian consists of the interacting impurities (H_{sys}), the noninteracting electron reservoirs (H_{res}), and their coupling which assumes the form of $H_{\text{sys-res}} = \sum_{\alpha\mu k} (t_{\alpha\mu k} \hat{a}_{\mu}^{\dagger} \hat{d}_{\alpha k} + \text{H.c.})$. Here \hat{a}_{μ}^{\dagger} and \hat{a}_{μ} denote the creation and annihilation opera-

*Electronic address: wjh@ruc.edu.cn

†Electronic address: xz58@ustc.edu.cn

‡Electronic address: yyan@ust.hk

tors for impurity state $|\mu\rangle$ (including spin, space, *etc.*), while $\hat{d}_{\alpha k}^\dagger$ and $\hat{d}_{\alpha k}$ are those for the α -reservoir state $|k\rangle$ of energy $\epsilon_{\alpha k}$. The influence of electron reservoirs on the impurities is taken into account through the overall reservoir spectral functions, $\Lambda_{\mu\nu}(\omega) \equiv \sum_{\alpha} \Lambda_{\alpha\mu\nu}(\omega) = \pi \sum_{\alpha k} t_{\alpha\mu k} t_{\alpha\nu k}^* \delta(\omega - \epsilon_{\alpha k})$, in the absence of applied chemical potentials. The HEOM that govern the dynamics of open system assume the form of [13]:

$$\begin{aligned} \dot{\rho}_{j_1 \dots j_n}^{(n)} = & - \left(i\mathcal{L} + \sum_{r=1}^n \gamma_{j_r} \right) \rho_{j_1 \dots j_n}^{(n)} - i \sum_j \mathcal{A}_{\bar{j}} \rho_{j_1 \dots j_n j}^{(n+1)} \\ & - i \sum_{r=1}^n (-)^{n-r} \mathcal{C}_{j_r} \rho_{j_1 \dots j_{r-1} j_{r+1} \dots j_n}^{(n-1)}, \end{aligned} \quad (1)$$

where the basic variables are the reduced system density operator $\rho^{(0)}(t) \equiv \text{tr}_{\text{res}} \rho_{\text{total}}(t)$ and auxiliary density operators (ADO), $\rho_{j_1 \dots j_n}^{(n)}(t)$; $n = 1, \dots, L$, with L denoting the terminal or truncated tier level. The Liouvillian of impurities, $\mathcal{L} \cdot \equiv \hbar^{-1} [H_{\text{sys}}, \cdot]$, may contain both e - e interaction and time-dependent external fields. The superoperators $\mathcal{A}_{\bar{j}}$ and \mathcal{C}_{j_r} are expressed by Eqs. (S1)–(S2) of Ref. [15]. Here, the individual index $j = (\sigma\mu m)$ corresponds to electron transfer to/from ($\sigma = +/ -$) the impurity state μ associated with a memory time γ_m^{-1} . The total number of distinct j -indexes involved is determined by the preset level of accuracy for decomposing reservoir correlation functions by exponential functions. Such a number draws the maximum tier level L_{max} at which the HEOM of Eq. (1) ultimately terminate [15].

The HEOM formalism is *nonperturbative*. It has been demonstrated that the hierarchy is self-contained at $L = 2$ level for noninteracting H_{sys} [13]. In practice, Eq. (1) needs to be truncated at a certain L , followed by a convergence test. Extensive numerical tests have affirmed that a relatively low truncation tier ($L \approx 4$) is usually sufficient to yield quantitatively converged results for weak and medium impurity-reservoir couplings. The HEOM approach has been applied to study the static and dynamical electron transport properties of quantum dot systems, with which some interesting phenomena have been revealed, such as the dynamical Coulomb blockade [16] and dynamical Kondo current [17].

For evaluation of dynamical variables of the impurities system, we focus on correlation function between two arbitrary dynamical operators, $\tilde{C}_{AB}(t) \equiv \langle \hat{A}(t) \hat{B}(0) \rangle = \text{tr}_{\text{total}} [\hat{A}(t) \hat{B}(0) \rho_{\text{total}}^{\text{eq}}(T)]$. Here, the Heisenberg operators and thermal equilibrium density operator $\rho_{\text{total}}^{\text{eq}}(T)$ are all defined in the total space. A linear response theory in the HEOM space is established (see Supplemental Materials [15] for details), based on which $\tilde{C}_{AB}(t)$ is retrieved exactly within the HEOM framework. Let $C_{AB}(\omega) \equiv \frac{1}{2} \int dt e^{i\omega t} \tilde{C}_{AB}(t)$, which satisfies the detailed balance relation of $C_{BA}(-\omega) = e^{-\hbar\omega/k_B T} C_{AB}(\omega)$. The system spectral function is obtained as $J_{AB}(\omega) \equiv \frac{1}{2\pi} \int dt e^{i\omega t} \langle \{\hat{A}(t), \hat{B}(0)\} \rangle = \frac{1}{\pi} (1 + e^{-\hbar\omega/k_B T}) C_{AB}(\omega)$. With $\hat{A} = \hat{a}_\mu$ and $\hat{B} = \hat{a}_\mu^\dagger$, it recovers the spectral func-

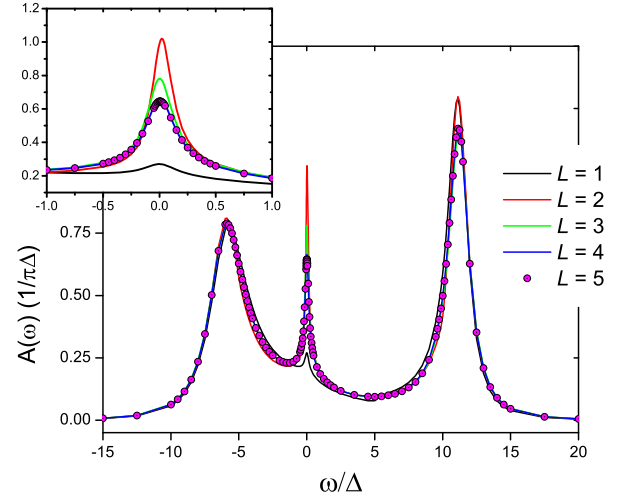


FIG. 1: (Color online). The spin-up or down spectral function of an asymmetric SIAM calculated by the HEOM approach at different truncation tiers. The inset magnifies the Kondo resonance peak at $\omega = 0$. The parameters adopted are $\epsilon_d = -5$, $U = 15$, $W = 10$, and $T = 0.075$ (in unit of Δ).

tion of the impurity state μ , *i.e.*, $A_\mu(\omega) \equiv J_{\hat{a}_\mu \hat{a}_\mu^\dagger}(\omega) = -\frac{1}{\pi} \text{Im} G_{\mu\mu}(\omega)$, which can be experimentally measured via angle-resolved photoemission spectroscopy [18] and scanning tunneling microscope [19]. Here, $G_{\mu\mu}(\omega)$ is the retarded Green's function.

For numerical demonstrations, consider first an asymmetric ($U \neq -2\epsilon_d$) SIAM system of $H_{\text{sys}} = \epsilon_d(\hat{n}_\uparrow + \hat{n}_\downarrow) + U\hat{n}_\uparrow\hat{n}_\downarrow$, where $\hat{n}_\mu = \hat{a}_\mu^\dagger \hat{a}_\mu$. The reservoir spectral function $\Lambda_{\mu\nu}(\omega) = \delta_{\mu\nu} \Delta W^2 / (\omega^2 + W^2)$ is adopted, where Δ is the effective impurity-reservoir coupling strength and W the reservoir band width. Such a model has been widely studied by various methods [20], including perturbation theory and NRG approach. Figure 1 shows the calculated impurity spectral function $A(\omega)$ via the HEOM approach up to the converged tier level. The parameters adopted are (in unit of Δ): $\epsilon_d = -5$, $U = 15$, $W = 10$, and $T = 0.075$. The calculation results display well-known features of SIAM: (i) The two resonance peaks resolved at around $\omega = \epsilon_d$ and $U + \epsilon_d$ represent the single-electron and two-electron occupancy states, respectively; (ii) The peak at the Fermi energy ($\omega = E_F \equiv 0$) highlights the presence of Kondo resonance under a low temperature; (iii) The sum rule $\int A(\omega) d\omega = 1$ is satisfied to numerical precision. The comparison in Fig. 1 demonstrates distinctly that the HEOM results converge rapidly with L for full energy range. This confirms the HEOM approach is capable of yielding quantitatively accurate dynamical properties at relatively small cost.

Figure 2 depicts the calculated $A(\omega)$ of a symmetric ($U = -2\epsilon_d$) SIAM with $T = 0.2\Delta$ and $W = 50\Delta$, from weak ($U = 0.5\pi\Delta$) to strong ($U = 6\pi\Delta$) e - e interaction. For comparison, we also show results obtained by using the full density matrix NRG method [21], where a self-energy scheme of Ref. [22] is employed, and the results

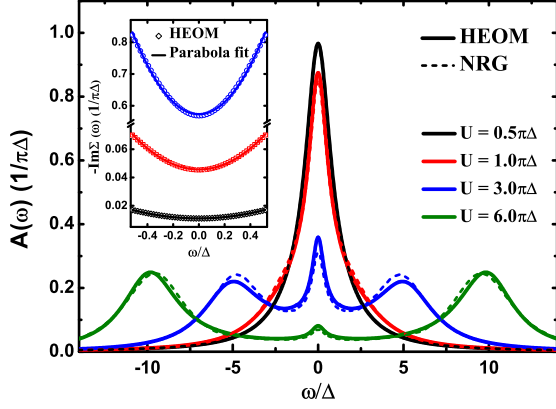


FIG. 2: (Color online). Spectral function of a symmetric SIAM calculated by HEOM and NRG at different e - e interactions. The inset shows the imaginary part of interaction self-energy calculated from HEOM at energy close to $\omega = 0$. Note the break of y axis in the inset.

are averaged over 8 different logarithmic discretizations [23]. Note that our NRG curves in Fig. 2 differ slightly from those in Ref. [24], due to the difference in lineshape of $\Lambda_{\mu\nu}(\omega)$ (Lorentzian versus constant). Apparently, the HEOM results agree quantitatively with the NRG counterparts for all e - e interaction strengths studied. In the weak ($U = 0.5$ and $1.0\pi\Delta$) and strong ($U = 6\pi\Delta$) interaction regimes, HEOM and NRG curves almost overlap with each other. Minor deviation is observed at an intermediate value ($U = 3\pi\Delta$), where the Hubbard peaks (around $\omega = \epsilon_d$ and $\epsilon_d + U$) from HEOM are at slightly higher energy than those from NRG. As is well known, NRG method tends to push the Hubbard peaks towards the lower energy, due to the Hilbert space truncation and log-Gaussian broadening. Therefore, the observed deviation takes place in the expected direction. The small differences near $\omega = 0$ for intermediate and strong interactions may result from the different numerical techniques adopted in NRG and HEOM approaches.

Highlighted in the inset of Fig. 2 are the imaginary part of interaction self-energy (scattered circles), exhibiting a parabolic lineshape near $\omega = E_F \equiv 0$ (solid lines). This is a clear indication of Fermi liquid character [20]. It has been proved by Luttinger [25] that for a symmetric SIAM at $T = 0$, the height of Kondo-resonance peak is exactly $1/\pi\Delta$, independent of U . In general, at finite T and U , it is expected that $A(\omega = 0) < 1/\pi\Delta$ for both asymmetric and symmetric SIAM systems [26], as affirmed in Fig. 1 and Fig. 2, respectively.

We extend the generic HEOM calculations to a parallel-coupled TIAM system, where the two-impurity Kondo effect emerges. We have now $H_{\text{sys}} = H_1 + H_2 + V_{12}$, with H_1 (H_2) being the SIAM Hamiltonian for the impurity 1 (2) and $V_{12} = t(a_{1\uparrow}^\dagger a_{2\uparrow} + a_{1\downarrow}^\dagger a_{2\downarrow} + \text{H.c.})$. Such a TIAM model has been realized experimentally via a double quantum dot system as sketched in Fig. 3(a), where the inter-dot coupling t is tuned by plunger gates [14].

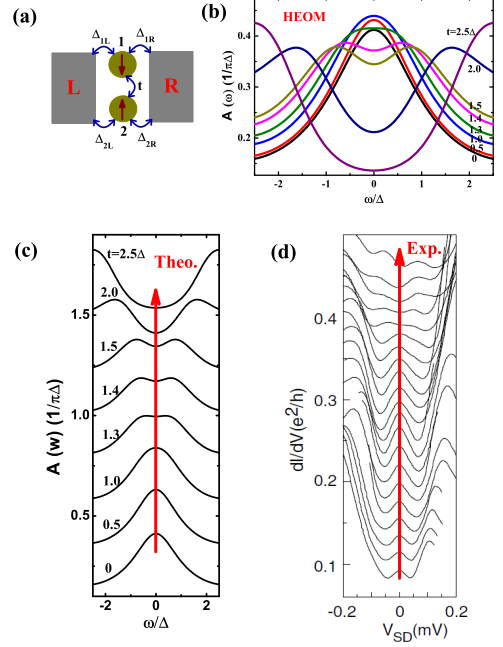


FIG. 3: (Color online). (a) Schematic diagram of a parallel-coupled TIAM system. (b) Spectral function of a symmetric TIAM consisting of two identical impurities, $A(\omega) = A_1(\omega) = A_2(\omega)$, at various inter-impurity coupling strengths t ranging from 0 to 2.5Δ . (c) HEOM results and (d) experimental measurement of $A(\omega)$ in Ref. [14] (Reprinted with permission), where the red arrows indicate the increasing direction of t .

An intriguing question is how the inter-impurity coupling would affect the Kondo signature. It is known that the t -coupling should induce a transition from a Kondo singlet of individual impurity to a singlet spin-state between two impurities. However, it remains unclear whether such a transition involves a critical point (quantum phase transition) or not. Jones *et al.* [27] studied a serial-coupled two-impurity system by carrying out pioneering NRG calculations on a Kondo model with an impurity-impurity exchange coupling term. Their results marked the transition by a non-Fermi liquid fixed (critical) point. Recent NRG calculations also found the critical point in a parallel-coupled two-impurity Kondo model [28]. However, such a quantum critical behavior is yet to be verified by experiments. In contrast, Chen *et al.* have observed a continuous crossover behavior in a parallel-coupled double quantum dot setup represented by Fig. 3(a) [14]. The apparent inconsistency between theory and experiment calls for quantitatively accurate numerical studies on more realistic models. For this purpose, we explore a TIAM by carrying out HEOM calculations to numerical convergence.

Figure 3(b) summarizes the calculated spectral functions of a TIAM consisting of two identical impurities, $A(\omega) \equiv A_1(\omega) = A_2(\omega)$, at various values of t . Other parameters are (in unit of Δ): $W = 2.5$, $U_1 = U_2 = 10$,

$\epsilon_1 = \epsilon_2 = -5$, and $T = 0.5$. For a symmetric TIAM, the differential conductance (dI/dV) is approximately proportional to $A(\omega)$ in linear response regime at low temperature [15]. Therefore, the HEOM calculated $A(\omega)$ can be compared directly to experimentally measured dI/dV of Ref. [14]; see Fig. 3(c) and (d), where red arrows indicate the increasing t . With Fig. 3(b)–(d), we demonstrate that the calculations well reproduce the essential experimental features: (i) The system undergoes a transition from a Kondo singlet involving individual impurity (characterized by the single-peaked lineshape) at $t < \Delta$, to the singlet spin-state between two impurities (characterized by the double-peaked lineshape) at $t > 1.5\Delta$; (ii) The transition exhibits a continuous crossover. As t increases from Δ , the single Kondo peak first broadens and approaches to its maximal height before it drops and splits into two; (iii) Beyond the crossover regime ($t > 1.5\Delta$), the separation between the two peaks increases rapidly with t , with each peak resembling the original unified one in both shape and width.

For a TIAM system, the nonzero t gives rise to an effective anti-ferromagnetic coupling, $J = 4t^2/U$, between the local spin moments at the two impurities. At a weak J , the two spin moments are nearly independent of each other, and the itinerant electrons screen the local spin at each impurity separately. In contrast, at a sufficiently strong J , singlet spin-states are formed, which span over both impurities. The absence of quantum phase transition in Fig. 3 might be due to the instability of quantum critical point under the chosen parameters, or caused by the charge transfer term V_{12} in our model. The latter may change the possible quantum phase transition to a continuous crossover [29, 30]. More comprehensive investigation is needed.

To summarize, the practicality of our developed hierar-

chical Liouville-space approach is demonstrated through studies on Anderson impurity models, where the key Kondo resonance and Fermi liquid features due to strong e - e interaction are accurately characterized. The HEOM approach can be straightforwardly extended to more general quantum impurity models without additional derivation and programming efforts. Besides the equilibrium dynamical observables, the HEOM approach is also capable of giving transient electronic response to external fields such as laser pulses or applied voltages [16, 17]. These make the HEOM approach a powerful tool for simulation of strongly correlated quantum impurity systems. We should point out that the HEOM calculations can be expensive at extremely low temperature or strong impurity-reservoir coupling, where a high truncation tier level is necessary to achieve quantitative convergence. It is however possible to reduce computational cost significantly by developing more suitable reservoir spectrum decomposition schemes. Once converged, the HEOM results can serve as benchmarks to calibrate various approximate but efficient numerical approaches, particularly the effective single-electron approaches, which are useful for studying more complex systems. Moreover, it is anticipated that HEOM would become a routine numerical solver for strongly correlated lattice systems within the framework of dynamical mean field theory [1].

This work is supported by the Hong Kong UGC (AoE/P-04/08-2) (YJY), NSF of China (Nos. 11074302, 11074303, 21103157, 21033008), Fundamental Research Funds for Central Universities (No. 2340000034) (XZ), Youth Innovation Funds from Ministry of Education of China (No. 2340000025) (XZ), Research Funds of Renmin University of China (No. 11XNJ026) (JHW), and China NKBRFSC (No. 2012CB921704) (NHT).

-
- [1] A. Georges, G. Kotliar, W. Krauth, and M. J. Rozenberg, *Rev. Mod. Phys.* **68**, 13 (1996).
 - [2] J. E. Hirsch and R. M. Fye, *Phys. Rev. Lett.* **56**, 2521 (1986).
 - [3] S. R. White, *Phys. Rev. Lett.* **69**, 2863 (1992).
 - [4] G. Vidal, *Phys. Rev. Lett.* **91**, 147902 (2003).
 - [5] K. G. Wilson, *Rev. Mod. Phys.* **47**, 773 (1975).
 - [6] R. Bulla, T. A. Costi, and T. Pruschke, *Rev. Mod. Phys.* **80**, 395 (2008).
 - [7] E. Khosravi, A.-M. Uimonen, A. Stan, G. Stefanucci, S. Kurth, R. van Leeuwen, and E. K. U. Gross, *Phys. Rev. B* **85**, 075103 (2012).
 - [8] K. S. Thygesen and A. Rubio, *Phys. Rev. B* **77**, 115333 (2008).
 - [9] S. Kurth, G. Stefanucci, E. Khosravi, C. Verdozzi, and E. K. U. Gross, *Phys. Rev. Lett.* **104**, 236801 (2010).
 - [10] P. W. Anderson, *Phys. Rev.* **124**, 41 (1961).
 - [11] J. Hubbard, *Proc. Roy. Soc. A* **276**, 238 (1963).
 - [12] P. A. Lee, T. M. Rice, J. W. Serene, L. J. Sham, and J. W. Wilkins, *Comments on Cond. Matter Phys.* **12**, 99 (1986).
 - [13] J. S. Jin, X. Zheng, and Y. J. Yan, *J. Chem. Phys.* **128**, 234703 (2008).
 - [14] J. C. Chen, A. M. Chang, and M. R. Melloch, *Phys. Rev. Lett.* **92**, 176801 (2004).
 - [15] Supplemental Materials.
 - [16] X. Zheng, J. S. Jin, and Y. J. Yan, *New J. Phys.* **10**, 093016 (2008).
 - [17] X. Zheng, J. S. Jin, S. Welack, M. Luo, and Y. J. Yan, *J. Chem. Phys.* **130**, 164708 (2009).
 - [18] A. Damascelli, Z. Hussain, and Z. X. Shen, *Rev. Mod. Phys.* **75**, 473 (2003).
 - [19] O. Y. Kolesnychenko, G. M. M. Heijnen, A. K. Zhuravlev, R. de Kort, M. I. Katsnelson, A. I. Lichtenstein, H. van Kempen, *Phys. Rev. B* **72**, 085456 (2005).
 - [20] A. C. Hewson, *The Kondo Problem to Heavy Fermions*, Cambridge University Press, Cambridge, 1993.
 - [21] A. Weichselbaum and J. von Delft, *Phys. Rev. Lett.* **99**, 076402 (2007).
 - [22] R. Bulla, A. C. Hewson, and T. Pruschke, *J. Phys.: Condens. Matter* **10**, 8365 (1998).
 - [23] W. C. Oliveira and L. N. Oliveira, *Phys. Rev. B* **49**,

- 11986 (1994).
- [24] A. Isidori, D. Roosen, L. Bartosch, W. Hofstetter, and P. Kopietz, Phys. Rev. B **81**, 235120 (2010).
 - [25] J. M. Luttinger, Phys. Rev. **121**, 942 (1961).
 - [26] K. Yamada, Prog. Theor. Phys. **53**, 970 (1975).
 - [27] B. A. Jones and C. M. Varma, Phys. Rev. Lett. **58**, 843 (1987); *ibid.*, Phys. Rev. B **40**, 324 (1989).
 - [28] G. Zaránd, C. H. Chung, P. Simon, and M. Vojta, Phys. Rev. Lett. **97**, 166802 (2006).
 - [29] O. Sakai, Y. Shimizu, and T. Kasuya, Solid State Commun. **75**, 81 (1990).
 - [30] I. Affleck, A. W. W. Ludwig, and B. A. Jones, Phys. Rev. B **52**, 9528 (1995).